Hopping conduction in p-type MoS2 near the critical regime of the metal-insulator transition

Tae-Eon Park, Joonki Suh, Dongjea Seo, Joonsuk Park, Der-Yuh Lin, Ying-Sheng Huang, Heon-Jin Choi, Junqiao Wu, Chaun Jang, and Joonyeon Chang

Citation: Applied Physics Letters **107**, 223107 (2015); doi: 10.1063/1.4936571
View online: http://dx.doi.org/10.1063/1.4936571
View Table of Contents: http://scitation.aip.org/content/aip/journal/apl/107/22?ver=pdfcov
Published by the AIP Publishing

Articles you may be interested in

Nb-doped single crystalline MoS2 field effect transistor
Appl. Phys. Lett. **106**, 173506 (2015); 10.1063/1.4919565

p-type doping of MoS2 thin films using Nb
Appl. Phys. Lett. **104**, 092104 (2014); 10.1063/1.4867197

Metal-insulator transition and conduction mechanism in dysprosium doped Bi 1.7 Pb 0.4 Sr 2 Ca 1.1 Cu 2.1 O 8 + δ system
J. Appl. Phys. **104**, 013919 (2008); 10.1063/1.2951955

Hopping conductivity in Cr-doped β - Fe Si 2 single crystals
J. Appl. Phys. **97**, 093706 (2005); 10.1063/1.1887831

Variable-range hopping conductivity in thin film of the ladder compound [Ca 1+δ Cu 2 O 3] 4
J. Appl. Phys. **94**, 5912 (2003); 10.1063/1.1603961

NEW Special Topic Sections
NOW ONLINE
Lithium Niobate Properties and Applications: Reviews of Emerging Trends
AIP Applied Physics Reviews

This article is copyrighted as indicated in the article. Reuse of AIP content is subject to the terms at: http://scitation.aip.org/termsconditions. Downloaded to IP: 128.32.121.22 On: Mon, 28 Dec 2015 23:02:19

Hopping conduction in p-type MoS_2 near the critical regime of the metal-insulator transition

Tae-Eon Park,[1] Joonki Suh,[2] Dongjea Seo,[1,3] Joonsuk Park,[4] Der-Yuh Lin,[5] Ying-Sheng Huang,[6] Heon-Jin Choi,[3] Junqiao Wu,[2] Chaun Jang,[1,a)] and Joonyeon Chang[1,7,a)]

[1]*Center for Spintronics, Korea Institute of Science and Technology, Seoul 136-791, South Korea*
[2]*Department of Materials Science and Engineering, University of California, Berkeley, California 94720, USA*
[3]*Department of Materials Science and Engineering, Yonsei University, Seoul 120-749, South Korea*
[4]*Department of Materials Science and Engineering, Stanford University, Stanford, California 94305, USA*
[5]*Department of Electronics Engineering, National Changhua University of Education, Changhua 50007, Taiwan*
[6]*Department of Electronics Engineering, National Taiwan University of Science and Technology, Taipei 10607, Taiwan*
[7]*Department of Nanomaterials Science and Engineering, Korea University of Science and Technology, Daejeon 305-350, South Korea*

(Received 3 August 2015; accepted 13 November 2015; published online 3 December 2015)

We report on temperature-dependent charge and magneto transport of chemically doped MoS_2, *p*-type molybdenum disulfide degenerately doped with niobium (MoS_2:Nb). The temperature dependence of the electrical resistivity is characterized by a power law, $\rho(T) \sim T^{-0.25}$, which indicates that the system resides within the critical regime of the metal-insulator (M-I) transition. By applying high magnetic field (~7 T), we observed a 20% increase in the resistivity at 2 K. The positive magnetoresistance shows that charge transport in this system is governed by the Mott-like three-dimensional variable range hopping (VRH) at low temperatures. According to relationship between magnetic-field and temperature dependencies of VRH resistivity, we extracted a characteristic localization length of 19.8 nm for MoS_2:Nb on the insulating side of the M-I transition. © *2015 AIP Publishing LLC*. [http://dx.doi.org/10.1063/1.4936571]

Layered transition metal dichalcogenides (LTMDs) receive significant research attention due to their potential applications in nanoelectronics and optoelectronics.[1–6] Recent studies on monolayer molybdenum disulfide (MoS_2), a direct band gap two-dimensional semiconductor with strong spin-orbit coupling,[7] have presented not only interesting physics such as valley Hall effect[8] and superconductivity,[9] but also promising electrical properties with high on/off ration (of $\sim 10^8$) and high effective mobility of electrons (up to 500 cm^2/V s).[2]

In order to realize MoS_2 based complementary bipolar devices, which are integral components for low-power, high-performance complementary logic applications,[10–12] both types of conduction in the MoS_2 should be realized. To further understand MoS_2's potential for the device applications, chemically doping in MoS_2 is required similar to traditional semiconductor technologies. *p*-type conduction of the MoS_2 further enables the access to spin polarized valence band, which is of much interest for emerging valleytronics.[7] However, most of the pristine MoS_2 devices are intrinsically *n*-type semiconductors owing hypothetically to sulfur vacancies and it has been hard to achieve *in situ* *p*-type doping of MoS_2 based devices until recently. A few groups have successfully demonstrated that stable *p*-type conduction in MoS_2 using niobium (Nb) as a substitutional cation, as Nb has indeed been theoretically suggested as an effective dopant for *p*-type doping of MoS_2.[13,14]

[a)]Authors to whom correspondence should be addressed. Electronic addresses: cujang@kist.re.kr and presto@kist.re.kr

Earlier studies on native *n*-type mono- and few-layer MoS_2 fabricated by both mechanical exfoliation and CVD growth methods, showed degraded effective mobility values.[15–21] For the CVD grown MoS_2 which usually shows lower effective mobility compared to mechanically exfoliated ones, intrinsic structural defects, including point defects, dislocations, grain boundaries, and edges, are observed via direct atomic resolution imaging, and a large amount of electronic trap states are observed from capacitance and AC conductance measurements.[21–23] In addition, charge and magnetotransport properties are being studied currently, in native few-layer MoS_2.[24]

On the contrary, electrical transport mechanism for chemically doped MoS_2 based devices are rarely studied. Although a report on *p*-type Nb doped MoS_2 (MoS_2:Nb) polycrystalline thin films grown by CVD demonstrated that the mobility is mainly limited by ionized impurity scattering by showing an increase in effective mobility with reduced doping densities,[14] there is still no elaborate charge transport data such as temperature dependent resistivity and magnetoresistance (MR) measurements. In this work, we report a significant insight into charge and magneto transport properties of *p*-type MoS_2:Nb. Based on the temperature-dependent resistivity, we found that our MoS_2:Nb systems are weakly disordered and remains in the critical regime of the metal-insulator (M-I) transition.[16,25,26]

The MoS_2:Nb single crystals were grown by the chemical vapor transport (CVT) method.[13] Figure 1(a) displays a high-resolution transmission electron microscope (TEM) image of MoS_2:Nb, showing the clear lattice fringes and the single

This article is copyrighted as indicated in the article. Reuse of AIP content is subject to the terms at: http://scitation.aip.org/termsconditions. Downloaded to IP: 128.32.121.22 On: Mon, 28 Dec 2015 23:02:19

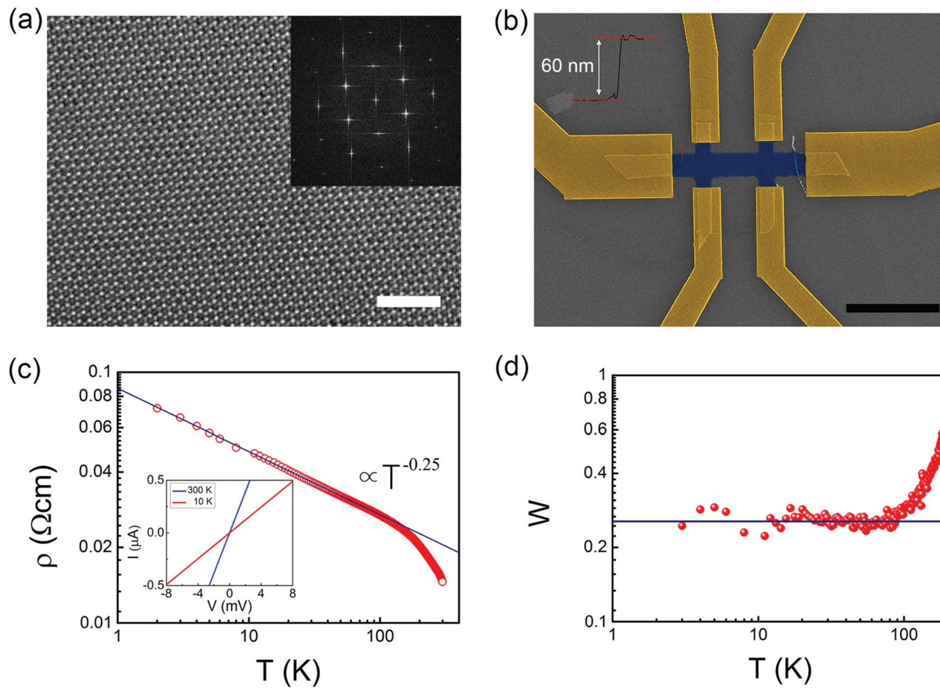

FIG. 1. Structural and charge transport of MoS_2:Nb. (a) Lattice resolved high-resolution TEM image of MoS_2:Nb (scale bar = 2 nm). The inset shows the corresponding FFT. (b) A false-color SEM image of a Hall-bar device on 60 nm thick-MoS_2:Nb flake (scale bar = 10 μm). (c) Log-log plot of the resistivity as a function of temperature. The solid line is a linear fit to the data (2 K < T < 100 K), showing a power-law divergence; $\rho(T) \sim T^{-0.25}$. The inset shows I-V characteristics of the MoS_2:Nb at 10 K and room temperature. (d) Log-log plot of the reduced activation energy $W = -T(\mathrm{d}\ln\rho/\mathrm{d}\ln T)$ at different temperatures. W is approximately constant below 100 K.

crystalline nature. The corresponding electron diffraction patterns show that the lattice spacing of 1.6 and 2.7 Å corresponding to the (110) and (100) planes, respectively, is consistent with reported values,[27] implying that Nb dopants are substitutionally incorporated into MoS_2 by replacing the Mo cations in the host lattice.[13] As-grown MoS_2:Nb crystals are also easily exfoliated similar to other TMDs. To determine the charge and magneto transport properties of chemically doped MoS_2, we fabricated Hall devices with MoS_2:Nb (see Fig. 1(b)). The thin flakes of the MoS_2:Nb were prepared on a Si substrate with a 300 nm-thick SiO_2 layer using the mechanical exfoliation. Then, a Hall bar configuration was defined using electron beam lithography (EBL) and XeF_2 gas etching. The multiple electrodes were defined through the second EBL followed by titanium/gold (5/100 nm) deposition and the lift-off process. The I-V curves of a MoS_2:Nb device at 300 K and 10 K are almost linear as shown in the inset of Fig. 1(c), indicating that good ohmic contacts between the metal electrodes and MoS_2:Nb have been obtained (supplementary Fig. S1).[28] The titanium/gold layer offers good ohmic contacts to the degenerated p-type MoS_2:Nb due to the narrow depletion width driven by heavily doping.[13,29] The thin flakes of MoS_2:Nb were found to exhibit a p-type behavior and hole mobility values are measured as $\sim$10 cm^2/V s with a corresponding carrier concentration of $\sim 10^{19}$ cm^{-3} at room temperature (see supplementary Fig. S2).[28]

The electrical resistivity as a function of temperature is shown in Fig. 1(c). The resistivity of p-type MoS_2:Nb increases with decreasing temperature, indicating that the charge transport does not follow the traditional metallic behaviour in spite of a high doping level (see supplementary Fig. S3).[28] As shown in Fig. 1(c), a log-log plot of the resistivity versus temperature is linear relation in a relatively wide temperature range, from 2 to 100 K, with a slope close to −0.25. The resistivity can be well defined by a power-law temperature dependence particularly below 100 K, $\rho(T) \propto T^{-0.25}$. For a three-dimensional (3D) conductor near the M-I transition, it is reported that the resistivity obeys a power-law temperature dependence as follows:[30]

$$\rho(T) \approx \left(\frac{e^2 p_F}{\hbar^2}\right)\left(\frac{k_B T}{E_F}\right)^{-\frac{1}{\eta}} \propto T^{-\beta}, \quad (1)$$

where e is the electron charge, p_F is the Fermi momentum, $\hbar$ is the reduced Planck constant, k_B is the Boltzmann constant, E_F is the Fermi energy, and $1 < \eta < 3$. The similar power-law temperature dependent behaviors have been observed in a variety of materials, such as n-doped Ge, doped single-wall carbon nanotube, camphor sulfonic acid (CSA) doped polyaniline (PANI), and PF6 doped polypyrrole (PPy).[31–34]

To explicitly describe the power-law temperature dependence of the resistivity, we also defined the reduced activation energy, W

$$W = -T\frac{d\ln\rho(T)}{dT} = -\frac{d\ln\rho}{d\ln T}, \quad (2)$$

which enables to determine which charge transport regime is mostly dominant among metallic, insulating, and boundary of the M-I transition.[32,34] Figure 1(d) shows the reduced activation energy at various temperatures on a log scale. We observed that W was approximately a constant value of 0.25 below 100 K. It clearly indicates that the charge conduction of thin flakes of MoS_2:Nb lies near the critical regime of the M-I transition below 100 K.

It is known that disorders generated during synthesis and doping process in heavily doped systems can provide the localization of states.[34] The larger magnitude of the disorder potential than the bandwidth leads to the localization of electronic states near E_F.[35,36] Although there is a finite density of states at E_F in such a system, the M-I transition can be driven by the disorder-induced localization.[36] From the power-law temperature dependence of resistivity and the constant value

This article is copyrighted as indicated in the article. Reuse of AIP content is subject to the terms at: http://scitation.aip.org/termsconditions. Downloaded to IP: 128.32.121.22 On: Mon, 28 Dec 2015 23:02:19

of W below 100 K, we demonstrate that our chemically doped MoS_2, p-type MoS_2:Nb system is weakly disordered and lies near boundary of the M-I transition.[32,33,36]

In the critical regime of the M-I transition, the temperature dependence of MR can be strongly related to the disorder interactions in the system. It can provide a useful clue to understand both the relevant scattering mechanism and the corresponding length scale.[33] We hence measured the Rxx while applying external magnetic field perpendicular to the surface of the Hall device. Figure 2(a) shows the MR at different temperatures (2–8 K). Below 8 K, p-type MoS_2:Nb exhibits the positive MR behaviour; i.e., Rxx increased with the applied magnetic field. A magnitude of MR, defined by $\Delta\rho/\rho_0 = [\rho(B) - \rho(0)]/\rho(0)$, at 7 T is 0.193 at 2 K and decreased to 0.023 at 8 K as shown in Fig. 2(a). For the detailed analysis of the positive MR behaviour, we plotted the differential MR ($d(\Delta\rho/\rho_0)/dB$) as a function of the applied magnetic field in Fig. 2(b). The positive MR was quadratic at low B and interestingly non-saturating linear at higher B marked in an arrow (see Fig. 2(a)). In the regular metals, the positive MR would saturate at high magnetic fields. The observed positive MR of the p-type MoS_2:Nb may be explained by the crossover from the critical regime to the insulating regime of the M-I transition. As the magnetic length (L_B) becomes comparable to the localization length (L_C) in the presence of applied magnetic field, the mobility edge of valence band can be shifted.[32,35] This shift of mobility edge causes the crossover from the critical behaviors to the insulating behavior.[32,35] The positive MR at low temperature originated from the mobility edge shift is a typical property for many disordered material systems.[32,35,37]

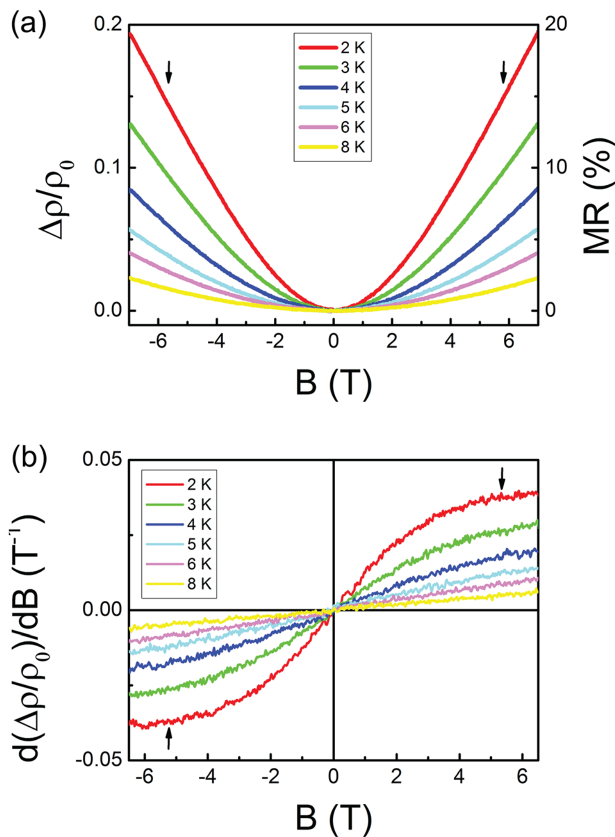

FIG. 2. Temperature dependent magnetoresistance ratio (MR) of MoS_2:Nb in the critical regime. (a) Transverse MR ($\Delta\rho/\rho_0$) of the MoS_2:Nb measured at $I = 100$ nA (213.7 Hz) with the four-terminal R_{xx} at low temperatures (2 K $\leq T \leq$ 8 K). (b) Differential MR ($d(\Delta\rho/\rho_0)/dB$) of the MoS_2:Nb as a function of temperature.

According to the theory of variable range hopping (VRH) mechanism proposed by Mott, the temperature dependence of the resistivity can be expressed as[38,39]

$$\rho(T) = \rho_0 \exp\left[\left(\frac{T_0}{T}\right)\right]^p, \tag{3}$$

where ρ_0 is a pre-factor, T_0 is a characteristic temperature, and the exponent p depends on the shape of the density of the states at the Fermi level; $p = 1/4$, 1/3, or 1/2 for 3D, 2D, and 1D systems, respectively. In Eq. (3), the exponent p is precisely deduced by the slope of $\ln[-d(\ln\rho)/d(\ln T)]$ versus $\ln T$, where $-d(\ln\rho)/d(\ln T) = p(T_0/T)^p$;[11,40,41] this analysis has been used in the observation of the crossover phenomenon in a 3D system. We plotted $[-d(\ln\rho)/d(\ln T)]$ as function of T on a log-scale at zero and high magnetic field ($B = 0$ and 7 T), as shown in the inset of Fig. 3. The inset of Fig. 3 shows a change of slope of $\ln[-d(\ln\rho)/d(\ln T)]$ versus $\ln T$ at high magnetic field below 8 K. The exponent p about 1/4 derived from the slope of $\ln[-d(\ln\rho)/d(\ln T)]$ versus $\ln T$ at 7 T below 8 K corresponds to 3D VRH conduction. Therefore, we believe that the charge transport is dominated by 3D VRH under an applied magnetic field at low temperatures. The magnetic field induced VRH conduction is more clearly presented in Fig. 3. The $\ln\rho(T)$ versus $T^{-1/4}$ curves at the zero magnetic field deviate from the linear plot, indicating the weaker temperature dependence. On the other hand, the $\ln\rho(T)$ versus $T^{-1/4}$ data follow a straight line at low temperatures (below 8 K) and the high magnetic field ($B = 7$ T), as shown in Fig. 3. It supports that the magnetic field induces the crossover from power-law temperature dependent behavior ($\rho \propto T^{-0.25}$) expected in the critical regime without

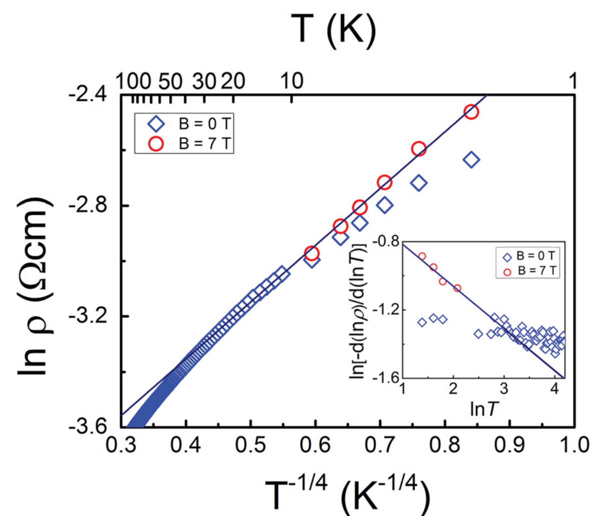

FIG. 3. The Mott variable range hopping transport at zero and high magnetic field of 7 T. The logarithmic plot of resistivity versus $T^{-1/4}$ in zero magnetic field (blue diamonds) and high magnetic field of 7 T (red circles). The solid line is fitted to the Mott variable range hopping model with 3D system in high magnetic fields ($2\text{ K} < T < 20\text{ K}$). The inset is the plot of $\ln[-d(\ln\rho)/d(\ln T)]$ versus $\ln T$, where a solid fitting line with high magnetic field of 7 T is used to extract the p-factor in Eq. (3).

This article is copyrighted as indicated in the article. Reuse of AIP content is subject to the terms at: http://scitation.aip.org/termsconditions. Downloaded to IP: 128.32.121.22 On: Mon, 28 Dec 2015 23:02:19

magnetic field and $\exp(T_0/T)^{1/4}$ behavior corresponding to 3D Mott VRH with magnetic field. We deduced a value of $T_0 = 17.4$ K from the straight line fit at 7 T below 20 K in Fig. 3. The small value of T_0 suggests that the system is very close to the M-I boundary and one can expect that VRH conduction is valid below the T_0. In fact, the $\ln\rho(T)$ versus $T^{-1/4}$ curves at the high magnetic field ($B = 7$ T) fell on a straight line below 20 K, as shown in Fig. 3.

We now discuss the localization length L_C of p-type MoS_2:Nb. The overlap of the localized state wave functions can be shrunk when the magnetic field is applied, resulting in an increase in the hopping length.[35] In this regard, the resistivity of the MoS_2:Nb in the insulating regime (3D VRH transport with $T_0 = 17.4$ K) is strongly related to the magnitude of the magnetic fields. The localization length can be estimated from the expression for magnetic-field and temperature dependence of the VRH resistivity as follows:[32,35]

$$\ln\left[\frac{\rho(B)}{\rho(0)}\right] = C\left[\left(\frac{L_C}{L_B}\right)\right]^4\left[\left(\frac{T_0}{T}\right)\right]^{\frac{3}{4}}, \quad (4)$$

where $C = (5/2016)$, $L_B = (c\hbar/eB)^{1/2}$ is the magnetic length, c is the velocity of light (≈ 9.5 nm at 7 T). We observed that the variation of $\ln[\rho(7\,\mathrm{T})/\rho(0\,\mathrm{T})]$ with $T^{-3/4}$ is a linear relationship at low temperatures as shown in Fig. 4. From the slope of straight line shown in Fig. 4, we estimated the localization length $L_C = 19.8$ nm from $T_0 \approx 17.4$ K and $L_B \approx 9.5$ nm at 7 T. In 3D Mott VRH conduction, T_0 is related to L_C and density of states at the Fermi level $N(E_F)$ as[40]

$$T_0 = \frac{18}{k_B} N(E_F) {L_C}^3. \quad (5)$$

We estimated a $N(E_F) = 1.5 \times 10^{21}$ states/eV·cm^3 of p-type MoS_2:Nb by the inserting the values of T_0 and L_C into Eq. (5).

In conclusion, our experimental results readily show that chemically doped MoS_2 exfoliated from single crystal of MoS_2:Nb lies at the M-I boundary. The resistivity of the MoS_2:Nb obeys a power-law temperature dependence, $\rho(T) \propto T^{-0.25}$, indicating that the system is in the near critical regime of M-I transition and weakly disordered. The positive MR at low temperatures reveals that the magnetic field can induce the crossover from the critical regime to the insulating regime. The hole transport under magnetic field can be taken into account by the VRH trough Nb induced localization states. The 3D VRH transport is supported by the temperature and field dependencies of the resistivity as well as the localization length estimated from the magnetic field dependence of the VRH resistivity. Our study clarifies the important role of the substitutional dopants as a source of the disorders in chemically doped MoS_2.

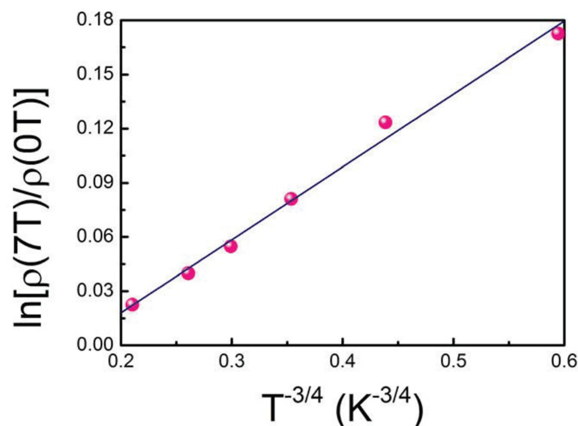

FIG. 4. Magnetic field dependence of the variable range hopping resistivity of MoS_2:Nb. Plot of $\ln[\rho(B)/\rho(0)]$ versus $T^{-3/4}$ for the MoS_2:Nb at $B = 7$ T, where a solid fitting line was used to extract the localization length.

This work was supported by KIST Institutional program (2V03730, 2E25450). The work at U. C. Berkeley was supported by the National Science Foundation under Grant No. DMR-1306601. The work at Yonsei University was supported by Nano. Material Technology Development Program through the National Research Foundation of Korea (NRF) funded by the Ministry of Education, Science and Technology (Grant No. 2014M3A7B4051594) and was supported and funded by the Agency for Defense Development (ADD).

[1]Q. H. Wang, K. Kalantar-Zadeh, A. Kis, J. N. Coleman, and M. S. Strano, Nat. Nanotechnol. **7**, 699 (2012).
[2]B. Radisavljevic, A. Radenovic, J. Brivio, V. Giacometti, and A. Kis, Nat. Nanotechnol. **6**(3), 147 (2011).
[3]K. F. Mak, C. Lee, J. Hone, J. Shan, and T. F. Heinz, Phys. Rev. Lett. **105**(13), 136805 (2010).
[4]A. Pospischil, M. M. Furchi, and T. Mueller, Nat. Nanotechnol. **9**(4), 257 (2014).
[5]B. W. H. Baugher, H. O. H. Churchill, Y. Yang, and P. Jarillo-Herrero, Nat. Nanotechnol. **9**(4), 262 (2014).
[6]J. S. Ross, P. Klement, A. M. Jones, N. J. Ghimire, J. Yan, D. G. Mandrus, T. Taniguchi, K. Watanabe, K. Kitamura, W. Yao, D. H. Cobden, and X. Xu, Nat. Nanotechnol. **9**(4), 268 (2014).
[7]D. Xiao, G.-B. Liu, W. Feng, X. Xu, and W. Yao, Phys. Rev. Lett. **108**(19), 196802 (2012).
[8]K. F. Mak, K. L. McGill, J. Park, and P. L. McEuen, Science **344**(6191), 1489 (2014).
[9]J. T. Ye, Y. J. Zhang, R. Akashi, M. S. Bahramy, R. Arita, and Y. Iwasa, Science **338**(6111), 1193 (2012).
[10]S. Chuang, C. Battaglia, A. Azcatl, S. McDonnell, J. S. Kang, X. Yin, M. Tosun, R. Kapadia, H. Fang, R. M. Wallace, and A. Javey, Nano Lett. **14**(3), 1337 (2014).
[11]Y. J. Zhang, J. T. Ye, Y. Yomogida, T. Takenobu, and Y. Iwasa, Nano Lett. **13**(7), 3023 (2013).
[12]M. Fontana, T. Deppe, A. K. Boyd, M. Rinzan, A. Y. Liu, M. Paranjape, and P. Barbara, Sci. Rep. **3**, 1634 (2013).
[13]J. Suh, T.-E. Park, D.-Y. Lin, D. Fu, J. Park, H. J. Jung, Y. Chen, C. Ko, C. Jang, Y. Sun, R. Sinclair, J. Chang, S. Tongay, and J. Wu, Nano Lett. **14**(12), 6976 (2014).
[14]M. R. Laskar, D. N. Nath, L. Ma, E. W. Lee, C. H. Lee, T. Kent, Z. Yang, R. Mishra, M. A. Roldan, J.-C. Idrobo, S. T. Pantelides, S. J. Pennycook, R. C. Myers, Y. Wu, and S. Rajan, Appl. Phys. Lett. **104**(9), 092104 (2014).
[15]D. Jariwala, V. K. Sangwan, D. J. Late, J. E. Johns, V. P. Dravid, T. J. Marks, L. J. Lauhon, and M. C. Hersam, Appl. Phys. Lett. **102**(17), 173107 (2013).
[16]H. Qiu, T. Xu, Z. Wang, W. Ren, H. Nan, Z. Ni, Q. Chen, S. Yuan, F. Miao, F. Song, G. Long, Y. Shi, L. Sun, J. Wang, and X. Wang, Nat. Commun. **4**, 2642 (2013).
[17]S. Ghatak, A. N. Pal, and A. Ghosh, ACS Nano **5**(10), 7707 (2011).
[18]A. M. van der Zande, P. Y. Huang, D. A. Chenet, T. C. Berkelbach, Y. You, G.-H. Lee, T. F. Heinz, D. R. Reichman, D. A. Muller, and J. C. Hone, Nat. Mater. **12**(6), 554 (2013).
[19]S. Najmaei, Z. Liu, W. Zhou, X. Zou, G. Shi, S. Lei, B. I. Yakobson, J.-C. Idrobo, P. M. Ajayan, and J. Lou, Nat. Mater. **12**(8), 754 (2013).
[20]H. Schmidt, S. Wang, L. Chu, M. Toh, R. Kumar, W. Zhao, A. H. Castro Neto, J. Martin, S. Adam, B. Özyilmaz, and G. Eda, Nano Lett. **14**(4), 1909 (2014).

This article is copyrighted as indicated in the article. Reuse of AIP content is subject to the terms at: http://scitation.aip.org/termsconditions. Downloaded to IP: 128.32.121.22 On: Mon, 28 Dec 2015 23:02:19

[21] W. Zhu, T. Low, Y.-H. Lee, H. Wang, D. B. Farmer, J. Kong, F. Xia, and P. Avouris, Nat. Commun. **5**, 3087 (2014).
[22] W. Zhou, X. Zou, S. Najmaei, Z. Liu, Y. Shi, J. Kong, J. Lou, P. M. Ajayan, B. I. Yakobson, and J.-C. Idrobo, Nano Lett. **13**(6), 2615 (2013).
[23] X. Chen, Z. Wu, S. Xu, L. Wang, R. Huang, Y. Han, W. Ye, W. Xiong, T. Han, G. Long, Y. Wang, Y. He, Y. Cai, P. Sheng, and N. Wang, Nat. Commun. **6**, 6088 (2015).
[24] A. T. Neal, H. Liu, J. Gu, and P. D. Ye, ACS Nano **7**(8), 7077 (2013).
[25] B. Radisavljevic and A. Kis, Nat. Mater. **12**(9), 815 (2013).
[26] B. W. H. Baugher, H. O. H. Churchill, Y. Yang, and P. Jarillo-Herrero, Nano Lett. **13**(9), 4212 (2013).
[27] Y.-H. Lee, X.-Q. Zhang, W. Zhang, M.-T. Chang, C.-T. Lin, K.-D. Chang, Y.-C. Yu, J. T.-W. Wang, C.-S. Chang, L.-J. Li, and T.-W. Lin, Adv. Mater. **24**(17), 2320 (2012).
[28] See supplementary material at http://dx.doi.org/10.1063/1.4936571 for details on the gate voltage dependence of electrical and magneto-transport properties.
[29] T.-E. Park, B.-C. Min, I. Kim, J.-E. Yang, M.-H. Jo, J. Chang, and H.-J. Choi, Nano Lett. **11**(11), 4730 (2011).
[30] A. I. Larkin and D. E. Khmel'nitskii, Sov. Phys. JETP **56**, 647 (1982).
[31] A. N. Iono and F. T. Poluprovodn, Sov. Phys. Semicond. **14**, 759 (1980).
[32] M. Reghu, Y. Cao, D. Moses, and A. J. Heeger, Phys. Rev. B **47**(4), 1758 (1993).
[33] J. Vavro, J. M. Kikkawa, and J. E. Fischer, Phys. Rev. B **71**(15), 155410 (2005).
[34] C. O. Yoon, M. Reghu, D. Moses, and A. J. Heeger, Phys. Rev. B **49**, 10851 (1994).
[35] R. Menon, C. O. Yoon, D. Moses, A. J. Heeger, and Y. Cao, Phys. Rev. B **48**(24), 17685 (1993).
[36] K. Lee, R. Menon, C. O. Yoon, A. J. Heeger, and Y. Cao, Phys. Rev. B **52**, 4779 (1995).
[37] W. Jiang, J. L. Peng, J. J. Hamilton, and R. L. Greene, Phys. Rev. B **49**(1), 690 (1994).
[38] N. F. Mott, Non-Cryst. Solids **1**, 1 (1968).
[39] N. F. Mott, *Metal-Insulator Transitions* (Taylor and Francis, London, 1974).
[40] S. I. Khondaker, I. S. Shlimak, J. T. Nicholls, M. Pepper, and D. A. Ritchie, Phys. Rev. B **59**, 4580 (1999).
[41] W. Paschoal, S. Kumar, C. Borschel, P. Wu, C. M. Canali, C. Ronning, L. Samuelson, and H. Pettersson, Nano Lett. **12**(9), 4838 (2012).

This article is copyrighted as indicated in the article. Reuse of AIP content is subject to the terms at: http://scitation.aip.org/termsconditions. Downloaded to IP: 128.32.121.22 On: Mon, 28 Dec 2015 23:02:19